Journal of Nuclear Materials 543 (2021) 152604

Contents lists available at ScienceDirect

Journal of Nuclear Materials

journal homepage: www.elsevier.com/locate/jnucmat

XPS study of external α-radiolytic oxidation of UO_2 in the presence of argon or hydrogen

N.L. Hansson[a,*], P.L. Tam[b], C. Ekberg[a], K. Spahiu[a,c]

[a] Nuclear Chemistry / Industrial Materials Recycling, Chalmers University of Technology, SE-412 96, Gothenburg, Sweden,
[b] Department of Industrial and Materials Science, Chalmers University of Technology, SE-412 96, Gothenburg, Sweden,
[c] Swedish Nuclear Fuel and Waste Management Co., SE-101 24, Stockholm, Sweden

ARTICLE INFO

Article history:
Received 30 June 2020
Revised 28 August 2020
Accepted 14 October 2020
Available online 19 October 2020

Keywords:
UO_2
radiolysis
hydrogen effect
oxidation
dissolution
x-ray photoelectron spectroscopy

ABSTRACT

UO_2 pellets exposed to 1.85 MBq and 3.30 MBq Am-241 sources with a 30 μm separation in solution were studied under Ar and H_2 atmospheres. The 1.85 MBq Am-241 source was shown to have a too low radiolytic production to cause any measurable change in UO_2 surface oxidation state. However, a significant oxidation was observed after exposure to the 3.30 MBq source under Ar atmosphere through the production of U(V), as seen from the U4f$_{7/2}$-peak deconvolution and valence band peak analysis. The H_2 atmosphere was shown to suppress the oxidation of the UO_2 pellet surface as well as the dissolution in both Milli-Q and $NaHCO_3$ solutions. The dissolved uranium concentration was reduced by a factor 10 under H_2 atmosphere as compared to the Ar atmosphere experiments.

1. Introduction

The release of radiotoxic species from a final geological nuclear waste repository is governed by the oxidative dissolution of the UO_2-matrix in the case of a canister failure. At the depths of a final geological repository (~500 m), the conditions are oxygen free and reducing [1]. In repositories built in granitic bedrock, as in the designs planned in Sweden, Canada and Finland, anoxic conditions are further ensured by the redox chemistry of the copper canister as well as with the surrounding biotite, magnetite and organic matter [2,3]. The UO_2 fuel matrix is highly insoluble in the U(IV) state, and the dissolution rate is therefore negligible under these conditions [4]. The main mechanism of dissolution is therefore through formation of locally oxidizing conditions near the fuel surface through water radiolysis. Even though water radiolysis produces both reducing and oxidizing species which are both radicals (H•, e^-_{aq}, HO_2•, O_2•, •OH) as well as molecular products (H_2, H_2O_2) [5], the redox conditions due to radiolysis are generally oxidizing at the immediate surface. This is due to the inertness of H_2 at temperatures close to room temperature [6]. The dominant oxidant of the UO_2 matrix under these conditions is H_2O_2 [7]. The oxidation and subsequent dissolution of the UO_2 matrix consequently leads to release of radiotoxic fission products and actinides, which are to a large extent (>95%) contained in the UO_2-matrix [8]. In the anoxic corrosion of the large iron inserts in the canister that occurs in contact with water, H_2 is produced. H_2 has been shown in several studies to protect the UO_2-surface of used fuel from oxidation, although the mechanism is not fully understood [9].

The kinetic activation of hydrogen can either occur at metallic ε-particles (Mo, Pd, Ru, Rh and Tc) or at surface-active UO_{2+x} sites. Several studies indicate that the activation occurs on UO_{2+x} sites through heterogeneous catalysis. In the work of King and Shoesmith, the activation of hydrogen on the pre-reduced electrode surface was delayed until oxidized U(IV)-U(V) sites were formed [9]. This was seen by an initial increase in the corrosion potential followed by a significant decrease, resulting in a corrosion potential ~200 mV below the potential under Ar atmosphere. The decrease in corrosion potential indicates reduction of the oxidized U(IV)-U(V) sites back to U(IV).

Sunder et. al. studied the effect of alpha radiolysis on UO_2-surfaces using ^{241}Am-sources in water at 100°C [10]. The α-sources irradiated a 30 µm thin water layer between the α-source and the UO_2-surface, achieved by placing Pyrex glass fibers (d=30 µm) in between. The experiments were conducted for 100 h under N_2 or H_2 atmospheres with Am-241 source strengths up to 14.8 MBq. The oxidation state of the surface was studied through X-ray photoelectron spectroscopy (XPS) measurements. The ratio U(VI)/U(IV) was determined through peak deconvolution of the U4f$_{7/2}$-peak into its U(VI) and U(IV) components [10]. It was shown that hydro-

* Corresponding author.
E-mail address: nikhans@chalmers.se (N.L. Hansson).

https://doi.org/10.1016/j.jnucmat.2020.152604

gen suppressed the oxidation of the UO_2-surface at 100°C. It was also noted that the surface became more reduced under hydrogen as the source strength was increased. However, the concentrations of dissolved uranium showed no discernable trend. This might be due to the large uncertainties in their Bromo-PADAP measurement of uranium concentrations. It was suggested by the authors that uranium colloids are a potential source of error, which combined with the large uncertainties in their concentration measurements could explain that no trend was observed in the evolution of uranium concentrations. Under N_2 atmosphere, the UO_2-surface oxidation state increased with increasing α-source strength.

The positions of the U(IV) and U(VI) components of the XPS-spectra have been reported by a number of authors as approximately 380 and 382 eV respectively [11-14]. Therefore, the 1.3 eV separation between the U(IV) and U(VI) components used by Sunder et. al. in their peak deconvolution in combination with a U(IV) position of ~380 eV would result in an overall higher oxidation state. As there was previously neither a pure U(V) reference compound nor conclusive studies that U(V) was a component in an oxidized UO_2-surface layer, U(V) was not included in the $U4f_{7/2}$-peak deconvolution process in many earlier studies [10,15,16]. In the more recent works of Kvashnina et. al. and Leinders et. al. the oxidation states in uranium oxide compounds was studied using high energy resolution fluorescence detection X-ray absorption near-edge structure spectroscopy (HERFD-XANES), showing that U(V) is a component in uranium oxides between UO_2 and UO_3, namely: U_4O_9, U_3O_7 and U_3O_8 [17,18]. The U(V)-component is therefore a crucial inclusion in the XPS analysis and $U4f_{7/2}$-peak deconvolution of any oxidized UO_2 surface. The inclusion of the U(V) component into the $U4f_{7/2}$-peak deconvolution process in the work of Sunder et. al. would have yielded a lower oxidation state. This is due to the close position of U(V) relative to the U(VI)-component, resulting from a rather low energy of the U(VI)-component in their work. The U(V) component would therefore occupy a significant fraction of the U(VI)-component envelope. This contributes to the rather large uncertainties in their UO_2 surface oxidation state measurements.

In this study, 1.85 and 3.30 MBq ^{241}Am-sources were used to expose a 30 µm layer of water between the sources and UO_2-surfaces to α-radiolysis at room temperature. The experiments were performed in both $NaHCO_3$ solution and Milli-Q water (18.2 MΩ•cm) to study the effect of $NaHCO_3$ on dissolution of oxidized UO_{2+x}. In the absence of $NaHCO_3$, the oxidized uranium is retained on the surface to a greater extent, and the degree of surface oxidation can be analyzed. The UO_2-samples exposed to the ^{241}Am-sources in Milli-Q water were subsequently analyzed using XPS, through which the C1s, U4f, O1s and valence regions were analyzed. The uranium oxidation state was determined by deconvolution of the $U4f_{7/2}$-peak into its U(IV), U(V) and U(VI) components as well as through analysis of the positions of the $U4f_{7/2}$ and $U4f_{5/2}$ peaks and their corresponding satellites [11]. Further analysis of the valence band region was also performed.

2. Materials and methods

2.1. UO_2 pellets and AmO_2 sources

Slightly enriched UO_2 pellets consisting of 98.0% ^{238}U and 2.0% ^{235}U were used in the experiments. Am-241 sources in the americium-oxide chemical form (Eckert & Ziegler) with α-activities 1.85 and 3.30 MBq respectively were used. The sources are covered by a 2 µm layer of pure gold to fix the radionuclide in the Au-matrix and prevent leakage. The dimensions of the AmO_2-powder compartment are Ø 15.5 × 0.4 mm. The sources are encapsulated in a SS AISI 304 frame exposing a cross-section Ø 11.5 mm.

2.2. Experimental setup

The surfaces of the pellets were polished using 600 & 2400 grit SiC grinding paper prior to the experiments. The pellets were subsequently cleaned in four washing steps consisting of 80 mL solutions with 50 mM $NaHCO_3$ (99.99+% Aldrich) in the first washing step, 10 mM $NaHCO_3$ in the second and third steps and 0 $NaHCO_3$ mM in the last step for 24 h in each washing step. Experiments were performed in Milli-Q water (18.2 MΩ•cm) and carbonate solutions. All experiments were conducted under room temperature (~298.15 K). The carbonate solution experiments were conducted in glass beakers with ~150 mL 10 mM $NaHCO_3$ solutions for 45 days and the Milli-Q experiments were conducted in plastic tubes with ~45 mL water for 11 days. An additional experiment was conducted with ~150 mL Milli-Q water for 45 days. The experimental setup for the experiments can be seen in Fig. 1. The beakers and tubes were placed inside stainless-steel autoclaves with a total internal volume of 450 mL (Parr Instruments Co., USA). In the $NaHCO_3$-experiments, a stainless-steel dip-tube was connected to the autoclave lid which allowed for sample outtakes using the overpressure inside the autoclave. The original autoclave designs were modified prior to the experiments by replacing the NPT connections by VCR ones to make the autoclaves more leak tight, minimizing the hydrogen leakage during the experiments. This was further achieved by using graphite gaskets, which deform as the autoclave is closed. The pellet washes and the experiments were conducted in an Inert Technology Glovebox with $p_{O2} \leq 1$ ppm. The pellets were transferred to the XPS using a transfer vessel which is compatible with the introduction chamber of the instrument.

2.3. Sample analysis

The dissolved uranium concentration was measured by inductively coupled plasma mass spectrometry (ICP-MS) (Thermo Scientific iCAP Q). ICP-MS samples were prepared using 0.5 M HNO_3 prepared from Merck suprapur 65% HNO_3 and the ICP-MS calibration was performed using ^{238}U standard in the range 0-50 ppb using 10 ppb ^{232}Th as internal standard. The detection limit is approximately 0.1 ppb for the analyzed elements.

2.4. XPS analysis

A PHI5000 VersaProbe III Microprobe XPS instrument was used in the surface measurements. The instrument is equipped with a monochromatic Al K-α x-ray source with energy 1486.6 eV [19], as well as with a dual charge compensation utilizing an electron neutralizer and an ion gun with negative and positive charge compensations respectively. To avoid surface contamination and/or chemical alteration after the carbonate wash or radiation exposure, the treated pellets were mounted to the sample plate and placed in a vacuum transfer vessel while in the glove box before transferred to XPS. The transfer vessel atmosphere is therefore the same as the glovebox, Ar with $p_{O2} \leq 1$ ppm. The binding energy scale was calibrated using the $Au4f_{7/2}$, $Ag3d_{5/2}$ and $Cu2p_{3/2}$ positions at 83.96±0.05, 368.21±0.05 and 932.63±0.05 eV respectively from argon ion sputtered gold, silver and copper pieces [20]. Surface composition was evaluated by a survey scan in the binding energy range between 0 and 1400 eV with an energy step size of 1.0 eV. The chemical states of uranium and oxygen, as well as the electronic structure, were studied in the narrow scan spectrum of the U4f (375-405 eV), O1s (525-540 eV) and valence band (-5-12 eV) regions with a step size of 0.1 eV. The spectrum was aligned with respect to the C1s signal at 284.8 eV stemming from adventitious carbon on the sample surfaces. The fitting routine of the peaks was performed using a 70% Gaussian-Lorentzian with a

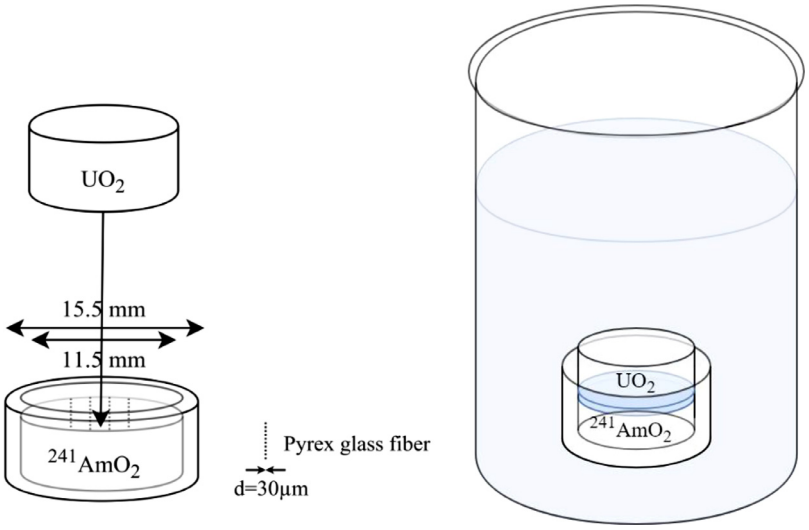

Fig. 1. The UO_2-pellet placed on top of the $^{241}AmO_2$ source with a separation of 30 µm achieved from Pyrex glass fibres.

Table 1
Characteristic features of the U(IV), U(V), U(VI) states and associated $U4f_{5/2}$-satellite positions.

Uranium oxidation state	$U4f_{7/2}$ position (eV) [11,22,23]	$U4f_{7/2}$-FWHM (eV) [23,24]	$U4f_{5/2}$-satellite shift (eV) [11,23-25]
U(IV)	380.0±0.2	1.8±0.3	6.9±0.2
U(V)	380.8±0.3	1.8±0.3	8.5±0.3
U(VI)	382.0±0.3	1.8±0.3	3.9±0.3, 9.8±0.3

Shirley background. A UO_2-sample was sputtered for 1 minute using a 2.0 kV Ar^+ beam with current density of 0.222 µA/mm^2 to remove surface oxidation and was used to define characteristics of a pure U(IV) state for the subsequent analyses. This made it possible to identify the FWHM of the pure U(IV) component as well as to verify the Gaussian-Lorentzian distribution in the fitting procedure. Literature values of the positions of the U(IV), U(V) and U(VI) $U4f_{7/2}$-peak components as well as the $U4f_{5/2}$-satellite can be seen in Table 1. It should be noted that binding energy position analysis should be used with caution and always be combined with other methods of spectrum analysis, such as peak deconvolution, satellite and valence band analysis. This is due to the fact that the binding energy scale is dependent on the charge correction, Fermi level position and work function, the latter which is quite substrate dependent [21].

3. Results and discussion

3.1. $NaHCO_3$ dissolution experiments

Two UO_2-pellets were exposed to the 3.30 MBq Am-241 source in a 10 mM $NaHCO_3$-solution under Ar and H_2 atmospheres respectively for ~45 days. The measured uranium concentrations as a function of time can be seen in Fig. 2. The solubility of U(IV)(am) is from the review of Neck and Kim [26] (accepted in the review of Ekberg and Brown [27]). The dissolved uranium concentration was quite stagnant during the first 15-day period, after which it increased quite rapidly under Ar atmosphere. The Ar atmosphere samples were ultracentrifuged and showed no evidence of colloids being present in the comparison with the non-ultracentrifuged samples. In the later stages of the experiment there were significantly lower amounts of uranium released under H_2 atmosphere, showing that H_2 had an inhibiting effect on the oxidative dissolution of uranium in the presence of carbonate. The solution volumes, duration and measured uranium concentrations at the end of the carbonate and Milli-Q experiments are shown in Table 2.

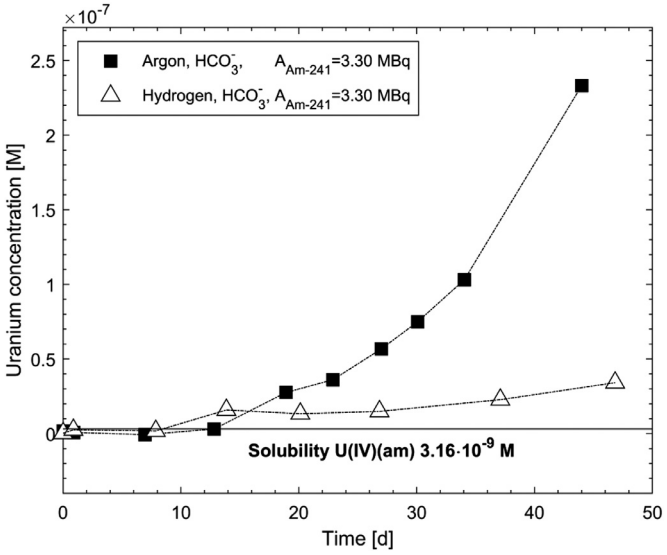

Fig. 2. Uranium concentrations in a 10 mM $NaHCO_3$ solution as a function of time in the 3.30 MBq Am-241 source exposure experiments under Ar and H_2 atmospheres. The solubility of U(IV)(am) is from the review of Neck and Kim [26].

3.2. ICP-MS results

Duplicate 11-days experiments under both 10 bar Ar and H_2 atmospheres in Milli-Q water using the 1.85 and 3.30 MBq Am-241 sources were conducted. The ICP-MS data from all experiments, including those in carbonate solutions discussed in the previous section are shown in Table 2. The UO_2-pellets that were exposed to the 1.85 MBq Am-241 source for 11 days under H_2 atmosphere gave dissolved uranium concentrations in the Milli-Q water below the detection limit of the ICP-MS measurement. The same was true for one of the two experiments of UO_2-pellets exposed to the 1.85

Table 2
Concentrations, volumes and times of all the external irradiation experiments.

A_{Am-241} [MBq]	Atmosphere	Volume [mL]	$NaHCO_3$ [M]	Time [d]	U-238 concentration [M]
1.85	H_2, 10 bar 1	45.09	0	11	- †
1.85	H_2, 10 bar 2	44.06	0	11	- †
1.85	Ar, 10 bar 1	45.15	0	11	- †
1.85	Ar, 10 bar 2	42.73	0	11	$5.09•10^{-8}$
3.30	H_2, 10 bar 1	44.43	0	11	$1.84•10^{-8}$
3.30	H_2, 10 bar 2	43.34	0	11	$3.53•10^{-8}$
3.30	Ar, 10 bar 1	43.45	0	11	$2.29•10^{-7}$
3.30	Ar. 10 bar 2	43.64	0	11	$3.19•10^{-7}$
3.30	Ar, 10 bar	153.01	0	45	$1.26•10^{-7}$
3.30	H_2, 10 bar	154.54	$10•10^{-3}$	47	$3.42•10^{-8}$
3.30	Ar, 10 bar	153.93	$10•10^{-3}$	44	$2.33•10^{-7}$

† Below detection limit of the ICP-MS measurement.

MBq Am-241 source for 11 days under Ar atmosphere, while the other pellet gave a dissolved concentration of $5.1•10^{-8}$ M. The 11-days Milli-Q experiments using the 3.30 MBq Am-241 source gave uranium concentrations that were higher than the corresponding concentrations in the carbonate experiments after roughly the same time period under both Ar and H_2 atmospheres (samples were taken at 13 & 14 days respectively, as shown in Fig. 2). This might be due to the significantly different solution volumes which affect the dissolution kinetics. However, this is somewhat unexpected, as the HCO_3^- ion forms a strong soluble complex with U(VI) [28]. Additionally, by dissolving the oxidized uranium the oxidation product cannot block further oxidation of the surface [7]. On the other hand, the inclusion of HCO_3^- would buffer the solution at pH ~8.34 (between pKa_1=6.35 and pKa_2=10.33) even at low concentrations. This buffering would prevent local acidification at the UO_2-surface due to the anodic dissolution reaction and could thereby possibly inhibit dissolution [29]. The same influence of HCO_3^- was observed in the work of de Pablo et. al., where the dissolution rate of UO_2 was initially slower in the presence of HCO_3^- as compared to that in Milli-Q water [30]. This was suggested to be due to radical scavenging by the HCO_3^- ion, thus reducing the radiolytic production of H_2O_2. This effect can however be hard to evaluate as HCO_3• is also a strong oxidant. Nevertheless, in the later stages of the experiments in the work of de Pablo et. al., the dissolved uranium concentration was higher in HCO_3^- solution, which corresponds well with the results found in this work [30].

The inclusion of $NaHCO_3$ increased the final dissolved uranium concentration by a factor two in the 45-days Ar atmosphere experiments. Additionally, comparing the 45-days Milli-Q Ar atmosphere experiment to the 11-days experiment, the total dissolved uranium content was a factor two higher at the end of the long experiment. At the end of the 45-days Milli-Q Ar atmosphere experiment, a 10 mL sample of the autoclave solution was taken out of the glove box and measured using a pH-electrode under air atmosphere. The measured pH was 6.9±0.5. The ionic strength of the sample was very low, adding uncertainty to the measurement. The sample was titrated with low concentration HNO_3 and showed no buffer capacity, indicating that there was no carbonate content present in the sample solution due to the washing procedure.

The experiments performed by Sunder et. al. were considerably shorter (100 h) than the ones performed in this work and were also performed under 100°C [10]. This makes their results somewhat difficult to compare to the ones in this work. The uncertainties in the Bromo-PADAP concentration measurements of Sunder et. al. are considerable, but some trends can be discerned. Under N_2 atmosphere, the uranium concentrations increased with increasing source strength. However, no significant difference in dissolved uranium concentrations under N_2 and H_2 atmospheres could be seen. In this work, the H_2 atmosphere significantly influenced the dissolved uranium concentrations as compared to the Ar atmosphere experiments by an order of magnitude, roughly 10^{-8} M under H_2, as compared to 10^{-7} M under Ar. The same was true in both Milli-Q and $NaHCO_3$-solutions. The dissolved uranium concentrations in this work are in the same order of magnitude under H_2 atmosphere as the ones obtained by Sunder et. al. at 100°C after an exposure time of 100 h. However, the dissolved amounts under Ar atmosphere in this work are significantly higher, by an order of magnitude.

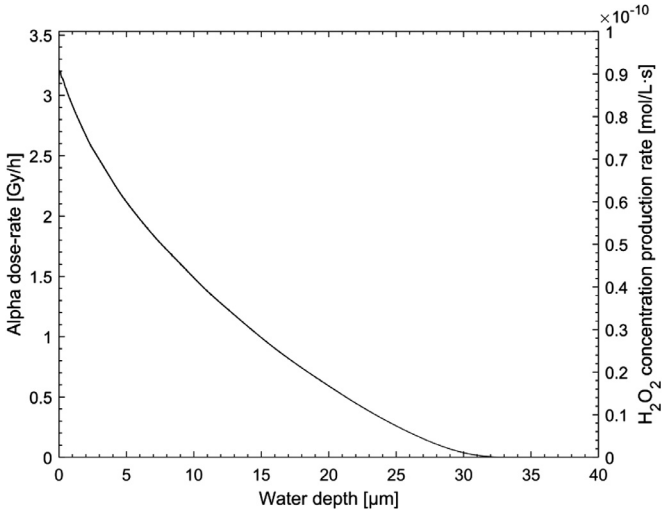

Fig. 3. Modelled α-dose-rate from the 3.30 MBq Am-241 source as a function of water depth perpendicular to the surface of the source.

3.3. Radiolytic oxidant production

Due to the lack of stopping power data for AmO_2, as well as in the uncertainty of the density of the AmO_2-powder in the source, UO_2 with 95% theoretical density is used as an approximation of the material. The ASTAR database combined with the CSDA approach and a geometric calculation model was used, as described in a previous work by our group [31]. The dose rate in solution perpendicular to the Am-241 source was calculated, where the attenuation in the 2 μm gold layer was taken into account. The gold layer had quite a large influence on the escape energy of the α-particles. As can be seen from Fig. 3, few α-particles have a range longer than 30 μm, and the UO_2-surface therefore receives a very small fraction of the total dose. The Pyrex glass threads are assumed to absorb less than 1% of the total dose and were not considered in the model.

The irradiated volume between the Am-241 source and the UO_2-surface is V_{irr} = (11.5 mm/2)^2•π•0.03 mm = 3.12 mm^3. Over

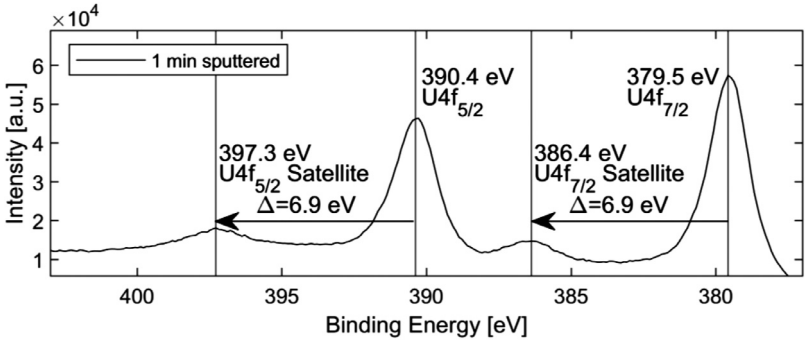

Fig. 4. The U4f spectrum of a washed UO_2 pellet after 1-minute argon ion sputtering.

an 11-day period, the total H_2O_2 production in V_{irr} exposed to the 3.30 MBq Am-241 source is $3.12 \cdot 10^{-5}$ mol/L. The total H_2O_2 production is modelled to find an approximate theoretical maximum dissolution assuming that all H_2O_2 causes oxidative dissolution of UO_2. A significant fraction of H_2O_2 will undergo decomposition on the UO_2 surface and will therefore not oxidize the surface [32], meaning that the theoretical maximum serves as a rough estimation of the total dissolved uranium concentration and is not a realistic one. If an appreciable fraction of the the locally produced H_2O_2 causes oxidation of the UO_2-matrix, the oxidative dissolution of the UO_2-matrix could produce locally more acidic conditions, enhancing the dissolution rate [29]. However, as the irradiation volume is considerably smaller than the total solution volume, diffusion will have a substantial effect on the chemical conditions close to the UO_2-surface. The modelling shows that the total dissolved uranium amount is higher than the radiolytic production of H_2O_2, indicating that the dissolution behaviour is influenced by dissolved oxygen or the presence of a pre-oxidized layer.

3.4. XPS-analysis

3.4.1. Ion-sputtered U(IV) state

A UO_2-pellet with low surface oxidation state was sputtered for 1 minute with the Ar^+-beam to remove the surface contamination and native oxide layer (see section 2.4 for further details). The U4f spectrum of the sputtered UO_2-surface can be seen in Fig. 4. Both the $U4f_{5/2}$- and $U4f_{7/2}$-peak positions after shifting the spectra with respect to the C1s-peak position at 284.8 eV are significantly lower than literature values by approximately 0.5 eV [11,22]. The spin orbit splitting of 10.9 eV between the two peaks however agrees very well with literature values [11,33]. This indicates a shift of the spectrum by 0.5 eV. The different $U4f_{7/2}$-peak position relative to the C1s-peak might be due to the dual charge compensation mechanism of the VersaProbe III instrument which differs from the compensation mechanisms of earlier models as well from that of other instruments. A very similar systematic peak shift can be seen in the work of Van den Berge et. al. which was also believed to be due to charging correction procedures [25]. The very distinct $U4f_{5/2}$- and $U4f_{7/2}$-satellites with a separation Δ=6.9 eV from their main peaks are indicative of a pure U(IV) oxidation state. The pure U(IV) signal in the $U4f_{7/2}$-envelope on the sputtered surface could be fitted well with a 70% Gaussian-Lorentzian, 1.7 eV FWHM peak at a binding energy of 379.5 eV. This corresponds well with FWHM literature values [24]. The value is however somewhat on the lower end, indicating a good resolution in the measurement [34]. The same parameters and systematic shift of the spectrum are used in the fitting procedure of the peak deconvolution process throughout this work.

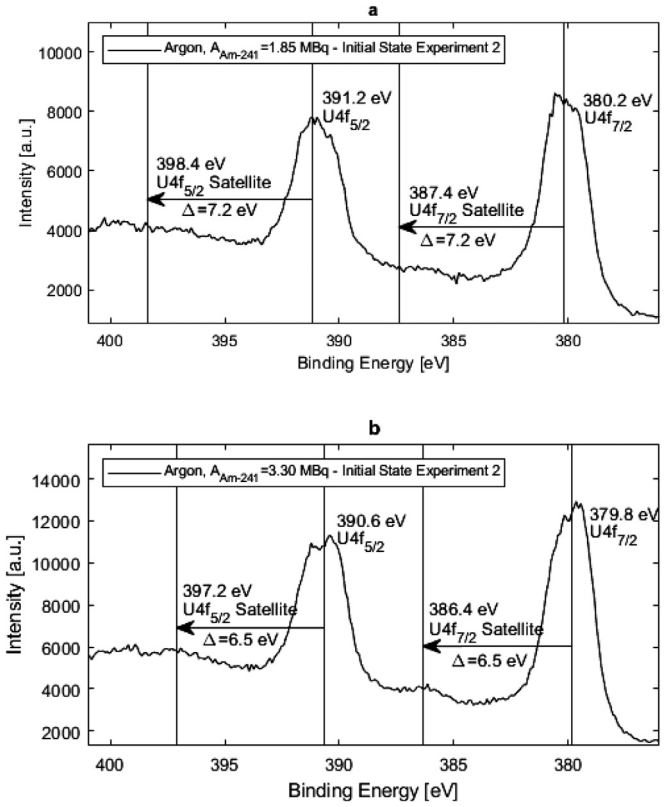

Fig. 5. U4f-spectra of the UO_2-pellets after the carbonate washing procedure, before exposure to the 1.85 (a) and 3.30 MBq (b) Am-241 sources under Ar atmosphere.

3.4.2. 11-days exposure under Ar atmosphere

The UO_2-pellets were measured by XPS after the initial washing process and were then subsequently exposed to the Am-241 sources. This allowed for a direct measurement of the change in oxidation state over the experiment. The initial U4f-spectra after the washing processes of the UO_2-pellets before exposure to the 1.85 and 3.30 MBq Am-241 sources are shown in Fig. 5a and Fig. 5b respectively**Error! Reference source not found.**. The $U4f_{7/2}$-peak positions are higher in energy than the sputtered UO_2 pellet, indicating a remaining contribution of oxidized uranium in the form of U(V) and/or U(VI) in the $U4f_{7/2}$-peak envelope after the washing procedure, despite the rather long washing durations. The satellite peak positions marked in the figures are approximate as their positions are affected by the contributions of U(IV), U(V) and U(VI) respectively. The more oxidation states existing in the main peak, the more spread out the satellite becomes. De Pablo et. al. studied the surface oxidation state of an initially oxidized UO_2-powder as

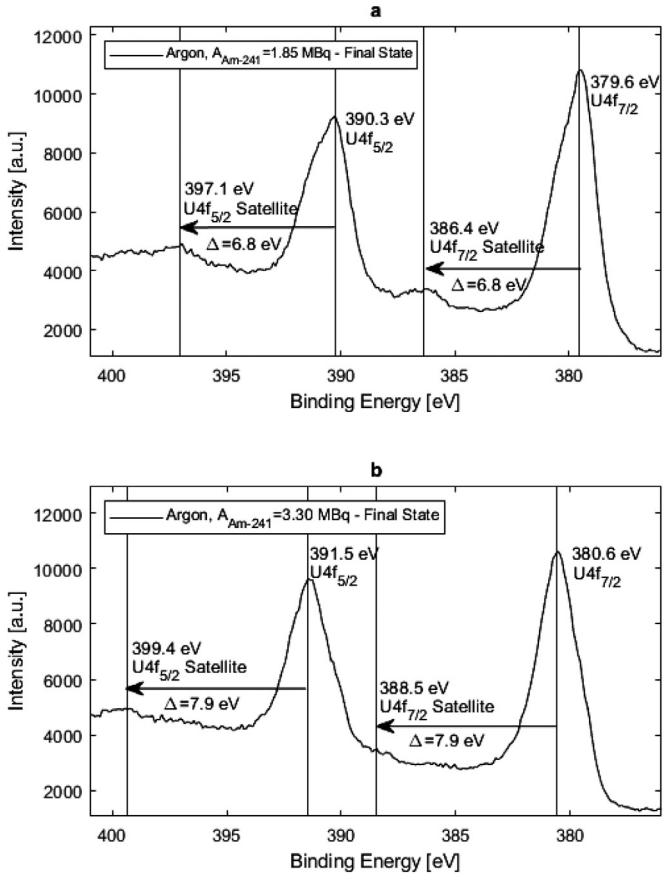

Fig. 6. U4f-spectra of the UO_2-pellets after 11-days exposure to the 1.85 (a) and 3.30 MBq (b) Am-241 sources under Ar atmosphere. Second experiment.

it was exposed to 10 mM carbonate solutions and found that after a 400-day exposure, the surface oxidation state was changed from $UO_{2.4}$ to $UO_{2.05}$. This shows that the oxidation above the $UO_{2.33}$-state, which would correspond to a surface with a U(VI)-component, is not required for the removal of oxidized uranium from the surface through carbonate complexation and dissolution of oxidized uranium [35]. It also shows that the complete dissolution of oxidized U(V) and U(VI) from a UO_{2+x} surface using carbonate washes is a very slow process. The rather high energy of the U4f$_{7/2}$ peak positions might therefore be due to insufficient washing times or conditions in the glove box that were too oxidizing (p_{O2} up to 1 ppm). It should be noted that carbonate does not act as a redox agent in the washing process and the apparent reducing effect of the surface is purely due to complexation and dissolution of oxidized uranium. As the transfer vessel was equipped with an O-ring and is tailor made for the sample inlet, the pellet surface is unlikely to have been oxidized during transfer to the XPS-instrument.

After exposing the pellets to the 1.85 and 3.30 MBq sources for 11 days in Milli-Q water under Ar atmosphere, the surfaces were analyzed again, and the final U4f-spectra are shown in Fig. 6. The pellet exposed to the 1.85 MBq Am-241 source has a significantly lower U4f$_{7/2}$-peak position than in the initial state, a shift of 0.6 eV. This indicates that the 1.85 MBq Am-241 source is too weak to compete with the dissolution of the pre-oxidized layer, resulting in almost a pure U(IV) signal at the end of the exposure period. However, the U4f$_{5/2}$- and U4f$_{7/2}$-satellites are not as distinct as on the surface of the sputtered sample, indicating some influence of the U(V) oxidation state. The U4f$_{7/2}$-peak deconvolution process into its U(IV), U(V) and U(VI) components as shown in Fig. 7a yields an equivalent oxidation state equal to $UO_{2.07}$.

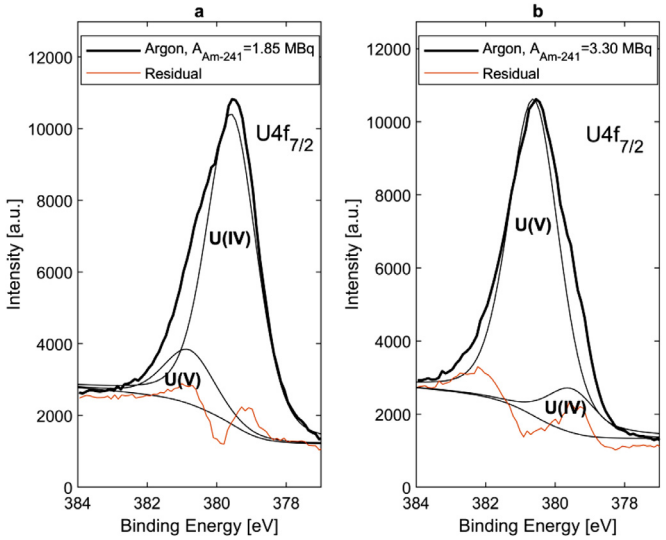

Fig. 7. Deconvolution of the U4f$_{7/2}$-peaks on the surface of the UO_2-pellets exposed to the (a) 1.85 and (b) 3.30 MBq Am-241 sources under Ar atmosphere for 11 days.

The U4f-spectrum of the pellet exposed to the 3.30 MBq Am-241 source (Fig. 6a) has a significant positive shift of the U4f$_{7/2}$-peak position. The peak deconvolution process shown in Fig. 7b yields an equivalent oxidation state of $UO_{2.44}$. The equivalent oxidation state is not believed to correspond to a single phase, but rather to an oxidized UO_{2+x} surface layer with a composition that probably varies with depth. The satellite positions in the spectrum of the UO_2 pellet exposed to the 3.30 MBq Am-241 source shown in Fig. 6b are somewhat approximate as the U4f$_{7/2}$-satellite is close to the tail of the U4f$_{5/2}$-peak and the U4f$_{5/2}$-satellite is rather broad. However, the satellites are within the 7.8-8.3 eV interval which is reported for the U(V) compounds in the review of Ilton & Bagus [11] and in the work of Gouder et. al. [23]. The corresponding O1s peaks of the Ar atmosphere experiments have not had a significant binding energy shift nor peak shape change in terms of FWHM. This is in agreement with the results of Santos et. al. where the lower applied potentials (up to -200 mV) resulted in an almost negligible O1s peak change [24].

3.4.3. 45 days 3.30 MBq Am-241 source exposure under Ar atmosphere

The 45-days exposure time under Ar atmosphere in Milli-Q water using the 3.30 MBq source resulted in a discernable shift of the U4f$_{7/2}$-peak position, shown in Fig. 8, as compared to the initial state samples. The position of the U4f$_{7/2}$-peak indicates a slightly lower extent of oxidation on the surface as compared to the 11-day experiment. The U4f$_{5/2}$-satellite is apparent, showing a position in good agreement with U(V).

The peak deconvolution of the U4f$_{7/2}$-peak of the 45-days Ar experiment can be seen in Fig. 9 below. The deconvolution yields a U(V)/U(IV) ratio of 1.88 which is equivalent with $UO_{2.33}$. This represents a lower oxidation state than for the 11-days experiment. The lower oxidation state is unexpected as the longer exposure time should allow for more radiolytic oxidation to occur. However, the solution volume is roughly a factor 3 larger as compared to the 11-days experiment (Table 2). The amount of H_2O_2 causing oxidative dissolution as compared to that undergoing decomposition is a function of solution volume, carbonate concentration as well as surface oxidation state composition [36]. H_2O_2 decomposition occurs at the UO_2 surface as well as in bulk solution, meaning that

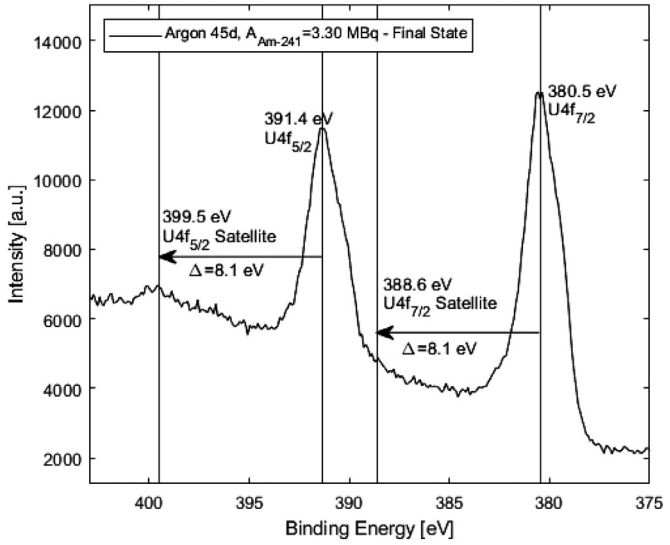

Fig. 8. The U4f-spectrum of a UO_2-pellet after 45-days exposure to the 3.30 MBq Am-241 source under Ar atmosphere.

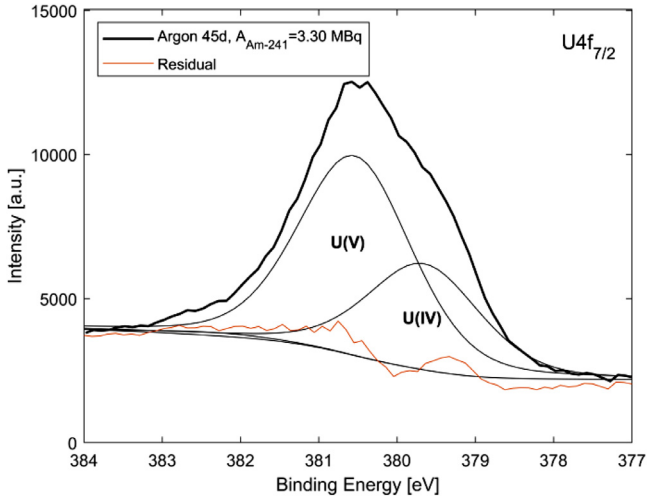

Fig. 9. Deconvolution of the $U4f_{7/2}$-peak from a UO_2-pellet after 45 days exposure to the 3.30 MBq Am-241 source under Ar atmosphere.

a larger solution volume would lead to a larger fraction H_2O_2 decomposing as compared to causing surface oxidation. The work of Zhu et. al. show that a mixed U(IV)/U(V) UO_2 surface is efficient at causing decomposition of H_2O_2, suggesting that a reversible U(IV)-U(V) redox reaction has a catalyzing effect on the surface decomposition reaction [36]. Taking the volume into account, the total dissolved amount of uranium at the end of the 45-days experiment was twice as high as in the 11-days experiment suggesting that the longer exposure times caused an overall higher oxidative dissolution of the UO_2 surface.

3.4.4. 11-days exposure under H_2 atmosphere

The UO_2-pellets were measured directly after the initial washing process as well as after being exposed to the Am-241 sources under H_2 atmosphere for 11-days. The initial U4f-spectrum after the washing process of the UO_2-pellets is shown in Fig. 10. Both initial U4f states correspond quite well with the previous reference states. Both the peak positions and their corresponding satellites indicate an almost pure U(IV) state. However, the slightly less clear satellite peaks as compared to the sputtered sample indicate an influence of U(V).

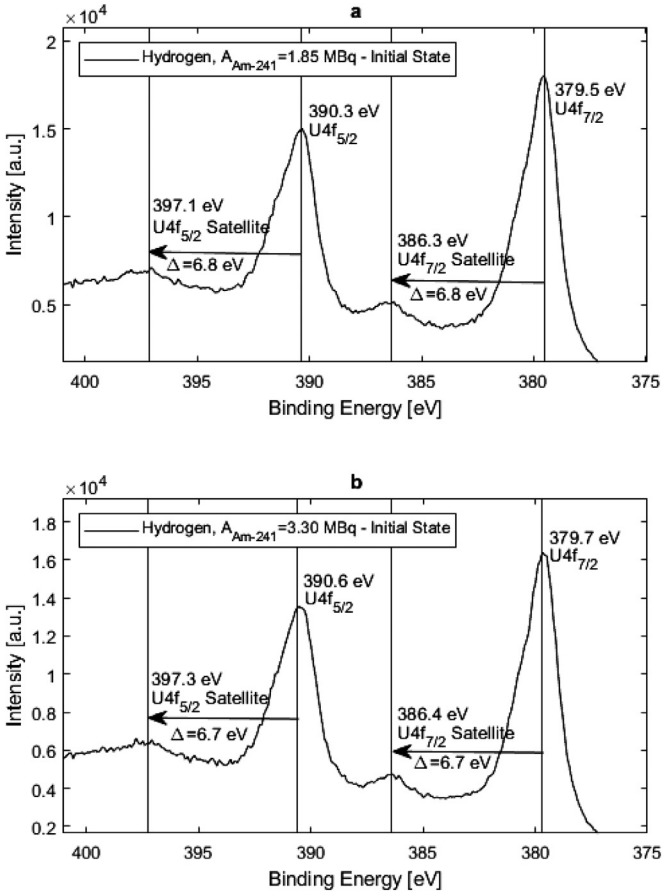

Fig. 10. U4f-spectra of the UO_2-pellets after the carbonate washing procedure, before exposure to the 1.85 (a) and 3.30 MBq (b) Am-241 sources under H_2 atmosphere.

The measured U4f-spectrum after exposure can be seen in Fig. 11. The spectrum is almost unchanged with respect to the initial state, with a small decrease in $U4f_{7/2}$-peak energy position of the pellet exposed to the 1.85 MBq Am-241 source. The results were replicated in a second experimental run with highly consistent results. It is likely that the long leaching periods allows for some of the initially oxidized U(V) & U(VI) to be released into solution up to levels close to or below the detection limit, as indicated by the ICP-MS measurements. The absence of change for both U4f7/2-peak and satellite position in the 3.30 MBq exposure indicate that the H_2 atmosphere has a suppressing effect on the radiolytic oxidation of the UO_2 surface. This is supported by the reduction in dissolved uranium concentration by an order of magnitude at the end of the H_2 atmosphere experiment of $3.5 \cdot 10^{-8}$ M as compared to $3.2 \cdot 10^{-7}$ M under Ar atmosphere.

In a study by Carbol et. al. where 10 wt% U-233 doped UO_2 was studied under H_2 atmosphere, a uranium concentration of ~$9 \cdot 10^{-12}$ M were found at the end of the 328 days experiment [37]. This indicates a significant protective effect of the H_2 atmosphere, suppressing any radiolytic oxidation. This shows a much stronger protective effect than the one observed in this work, where there were several orders of magnitude higher dissolved uranium concentrations.

3.4.5. Valence band region

The valence band region of the UO_2 pellets before and after exposure to the 1.85 & 3.30 MBq sources for 11 days under Ar and H_2 atmospheres can be seen in Fig. 12 and Figure 13 respectively. The area ratio between the $O2p_{3/2}$ and U5f states in the initial state

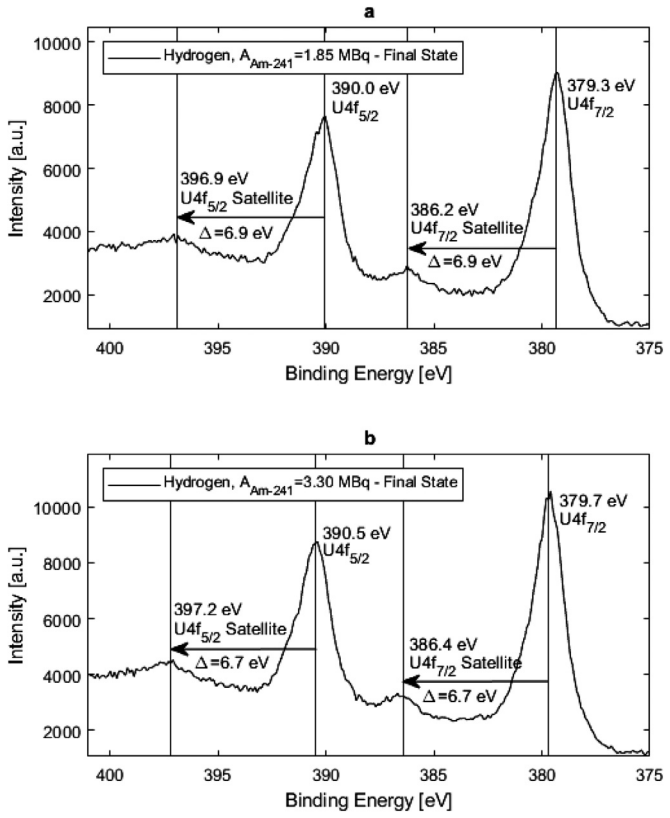

Fig. 11. U4f-spectra of the UO_2-pellets after 11-days exposure to the 1.85 (a) and 3.30 MBq (b) Am-241 sources under H_2 atmosphere. Second experiment.

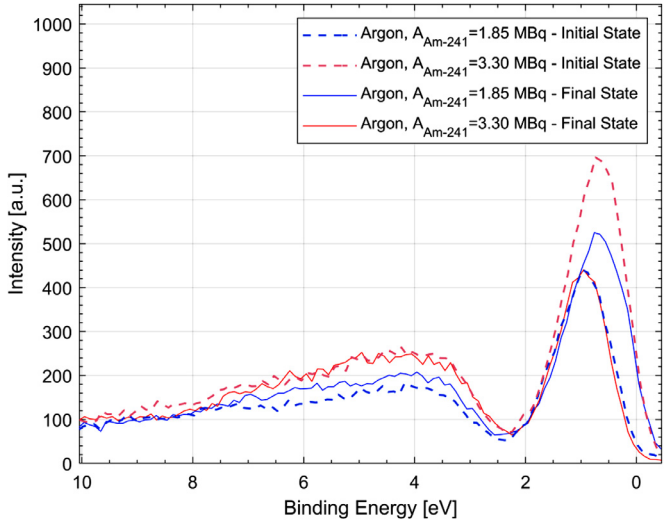

Fig. 12. Valence band region of the pellets before and after exposure to the 1.85 and 3.30 MBq Am-241 sources under Ar atmosphere.

is approximately ~1.0, as shown in Table 3. All reported O2p$_{3/2}$ and U5f state area ratio values are after the Shirley background subtraction. In the final state under Ar atmosphere, the O2p$_{3/2}$ to U5f state area ratios are 1.1 and 1.9 after exposure to the 1.85 and 3.30 MBq sources respectively. This indicates an almost negligible change in the O2p$_{3/2}$ and U5f electron structure after exposure to the 1.85 MBq source and a significant change in the electron distribution after exposure to the strong source. The more oxidized UO_2 pellet therefore has less electrons in the U5f-orbital and/or more electrons in the O2p-orbital. The U5f-FWHM of the pellet exposed

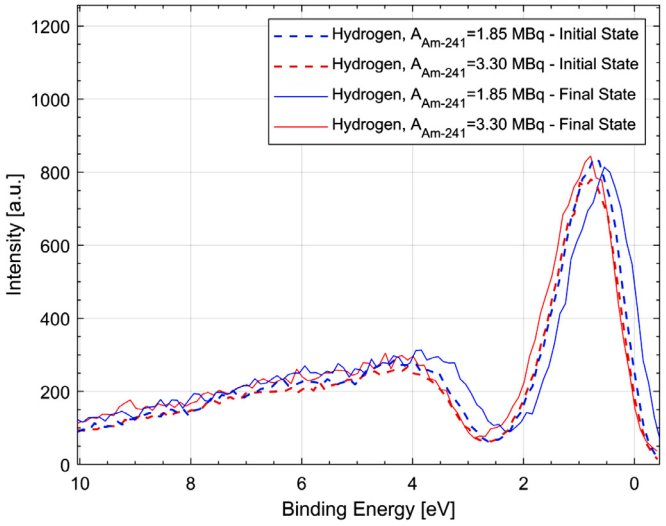

Fig. 13. Valence band region of the pellets exposed to the 1.85 and 3.30 MBq Am-241 sources under H_2 atmosphere for 11 days.

to the 3.30 MBq source for 11 days under Ar atmosphere goes from an initial value of 1.28 eV to a final one of 1.13 eV. This agrees quite well with the U5f-FWHM of pure U_2O_5 (i.e. pure U(V)) in the work of Gouder et. al. of 1.19 eV [23], supporting the notion of a significant U(V) component on the surface. The U5f-FWHM at the end of the 45-days experiment is very similar of 1.11 eV.

In the exposure under H_2 atmosphere, the area ratios of O2p to U5f-states are quite consistent over the experiment as shown in Fig. 13, of about ~1.0. This indicates a negligible change in surface oxidation state. This is supported by the consistent FWHM of the U5f-peaks in the initial and final states which are approximately ~1.4 eV. This is close to the FWHM of the U5f-peak on the sputtered sample, of 1.45 eV. These values are in good agreement with the FWHM of the pure U(IV) 5f-peak in the work of Gouder et. al. of 1.46 eV [23]. The researchers state that the pure U(V) component has a smaller U5f-FWHM and intensity than a mixture of U(IV) and U(VI). The results in their work indicate that the oxidation mechanism of UO_2 goes via a U(V) component and not directly to the formation of U(VI). This has been reported in several other studies, however, these studies are primarily of SIMFUEL, which contains RE(III), affecting the redox reactivity of the UO_2 matrix [24,36,38]. The oxidation from U(IV) to U(V) is supported by the results in this work as a substantial U(V) component was found in the U4f$_{7/2}$-peak deconvolution process of the final state on the UO_2-pellets exposed to the 3.30 MBq source for 11 and 45 days under Ar atmosphere (Fig. 7 & Fig. 9). These states also had significantly smaller U5f-FWHM and reduced intensities. The ratio between the U5f state and the O2p valence band for all the oxidized surfaces are ~1.9, while in the initial state the ratio is close to 1. The summarized O2p and U5f state results from all experiments are shown in Table 3.

4. Conclusion

The H_2 atmosphere had a significant impact on the surface oxidation of a UO_2-pellet after exposing a 30 μm water layer adjacent to the pellet surface to a 3.30 MBq Am-241 source. The H_2 atmosphere also suppressed the oxidative dissolution of uranium, giving an order of magnitude lower measured uranium concentrations at the end of the 11- and 45-days experiments in Milli-Q and $NaHCO_3$-solutions as compared to under Ar atmosphere. Exposing the UO_2-pellets to the 1.85 MBq Am-241 source caused no observable surface oxidation under neither atmosphere as compared to

Table 3
U5f and $O2p_{3/2}$ peak positions and FWHMs from the XPS-measurements.

Condition	U5f position [eV]	FWHM U5f [eV]	$O2p_{3/2}$ position [eV]	Area ratio ($O2p_{3/2}$ /U5f)
Ion-sputtered	0.8	1.45	4.1	1.0
Chemical washed	0.8	1.30	4.1	0.9
Ar atmosphere				
1.85 MBq – 11 days	0.7	1.35	4.0	1.1
3.30 MBq – 11 days	0.9	1.13	4.4	1.9
3.30 MBq – 45 days	0.9	1.11	3.4	1.9
H_2 atmosphere				
1.85 MBq – 11 days	0.5	1.45	3.9	1.0
3.30 MBq – 11 days	0.8	1.40	4.5	0.8

the initial states. The exposure to this source gave a somewhat lower $U4f_{7/2}$-peak position as compared to the initial states, suggesting a more significant effect of dissolution of pre-oxidized uranium. However, the amount of dissolved uranium at the end of the 1.85 MBq source exposures is very low, or even below the detection limit of the ICP-MS measurement (Table 2), suggesting that very little surface oxidation occurs. The 3.30 MBq source resulted in a significant oxidation under Ar atmosphere in the form of a substantial U(V) component. This was also shown by the small FWHM of the U5f-peak, indicative of a minor U(IV) and U(VI) contribution. The results support the claim that UO_2 does not oxidize directly from U(IV) to U(VI), but through the formation of U(V), without having a simultaneous mixed U(IV) and U(VI) oxidation state.

The results of this work indicate that the much stronger influence of hydrogen atmosphere on the pellet surface reduction noted in the work of Sunder et al. is partially due to thermally activated hydrogen, contributing to chemical reduction of U(VI) to U(IV) at 100°C [10]. Ekeroth et al. reported a slow reduction of U(VI) by dissolved hydrogen at 74-100°C [39], while no reduction in bulk solution was observed in another work carried out at 70°C [40]. In this work, carried out at room temperature, i.e. when dissolved hydrogen is expected to be chemically inert, the effect of dissolved hydrogen on preventing surface oxidation by alpha radiolysis is apparently a result of the interaction of ionizing radiation with water adsorbed on the surface of actinide oxides, the exact mechanism of which requires dedicated interfacial radiolysis studies. In this case, in addition to standard radiolytic processes, energy, charge or matter can be transferred through the interface, while catalytic or steric effects can alter the decomposition or reactivity of adsorbed molecules. Similar studies claiming recombination of alpha radiolysis products have been reported in the literature. The results of a radiolytic gas generation study on NpO_2(s) doped with 0.7 % ^{244}Cm in the presence of moisture (up to 8 wt% water), show that the gas generation quickly reaches a steady state plateau at relatively low total pressures [41]. The plateau is interpreted by the authors as clear evidence of a significant back reaction (i.e. the recombination of the radiolytic products O_2 and H_2 to water), where the forward reaction (radiolytic decomposition of water) is equal to the back reaction; a behaviour noticed by the authors also in other actinide systems. Haschke et al. observed a pressure decrease in a 2:1 (D_2 + O_2) gas mixture over $^{239}PuO_2$(s) at 25 °C, which was interpreted as being caused by the catalytic formation of water on the surface of PuO_2(s) [42]. The role of α-radiation in the interfacial processes involved in both these studies has not been discussed in the original publications, but its influence cannot be excluded [43]. It is difficult from our tests to draw any conclusions about the mechanism of the recombination reactions between radiolytic oxidants and hydrogen that we observe as absence of surface oxidation at room temperature, but it cannot be excluded that surface mediated processes contribute to the obtained results.

Declaration of Competing Interest

The authors declare that they have no known competing financial interests or personal relationships that could have appeared to influence the work reported in this paper.

CRediT authorship contribution statement

N.L. Hansson: Conceptualization, Methodology, Software, Formal analysis, Investigation, Writing - original draft, Visualization. **P.L. Tam:** Formal analysis, Investigation, Resources, Writing - review & editing. **C. Ekberg:** Writing - review & editing, Supervision. **K. Spahiu:** Conceptualization, Writing - review & editing, Supervision.

Acknowledgements

Svensk Kärnbränslehantering AB, SKB is greatly acknowledged for funding this research.

References

[1] S. Sunder, D.W. Shoesmith, Chemistry of UO 2 fuel dissolution in relation to the disposal of used nuclear fuel, 1991 Atomic Energy of Canada Ltd.
[2] L. Johnson, et al., The disposal of Canada's nuclear fuel waste: A study of post-closure safety of in-room emplacement of used CANDU fuel in copper containers in permeable plutonic rock. Volume 2: Vault Model, 1996 Atomic Energy of Canada Ltd.
[3] M. Kolář, F. King, Modelling the consumption of oxygen by container corrosion and reaction with Fe (II), in: MRS Proceedings, Cambridge Univ Press, 1995.
[4] D. Rai, M. Yui, D.A. Moore, Solubility and solubility product at 22 C of UO 2 (c) precipitated from aqueous U (IV) solutions, Journal of Solution Chemistry 32 (1) (2003) 1–17.
[5] A.O. Allen, The radiation chemistry of water and aqueous solutions, van Nostrand New York, 1961.
[6] G. Sattonnay, et al., Alpha-radiolysis effects on UO 2 alteration in water, Journal of nuclear materials 288 (1) (2001) 11–19.
[7] E. Ekeroth, O. Roth, M. Jonsson, The relative impact of radiolysis products in radiation induced oxidative dissolution of UO2, Journal of Nuclear Materials 355 (1-3) (2006) 38–46.
[8] L. Johnson, D. Shoesmith, Spent fuel, Radioactive waste forms for the future, 1988.
[9] F. King, D. Shoesmith, Electrochemical studies of the effect of H2 on UO2 dissolution, 2004 SKB Technical Report TR-04-20, Swedish Nuclear Fuel and Waste Management Co.
[10] S. Sunder, G.D. Boyer, N.H. Miller, XPS Studies of UO2 oxidation by alpha radiolysis of water at 100°C, Journal of Nuclear Materials 175 (3) (1990) 163–169.
[11] E.S. Ilton, P.S. Bagus, XPS determination of uranium oxidation states, Surface and Interface Analysis 43 (13) (2011) 1549–1560.
[12] Y.A. Teterin, et al., XPS study of ion irradiated and unirradiated UO2 thin films, Inorganic chemistry 55 (16) (2016) 8059–8070.
[13] L. Cox, J. Farr, 4f binding-energy shifts of the light-actinide dioxides and tetrafluorides, Physical Review B 39 (15) (1989) 11142.
[14] E.S. Ilton, et al., Mica surfaces stabilize pentavalent uranium, Inorganic chemistry 44 (9) (2005) 2986–2988.
[15] R. Delobel, et al., X-ray photoelectron spectroscopy study of uranium and antimony mixed metal-oxide catalysts, Journal of the Chemical Society, Faraday Transactions 1: Physical Chemistry in Condensed Phases 79 (4) (1983) 879–891.

[16] N. McIntyre, et al., Chemical information from XPS—applications to the analysis of electrode surfaces, Journal of Vacuum Science and Technology 18 (3) (1981) 714–721.
[17] K. Kvashnina, et al., Chemical state of complex uranium oxides, Physical review letters 111 (25) (2013) 253002.
[18] G. Leinders, et al., Evolution of the uranium chemical state in mixed-valence oxides, Inorganic chemistry 56 (12) (2017) 6784–6787.
[19] T.M. Willey, et al., Rapid degradation of alkanethiol-based self-assembled monolayers on gold in ambient laboratory conditions, Surface Science 576 (1) (2005) 188–196.
[20] M. Seah, Summary of ISO/TC 201 Standard: VII ISO 15472: 2001—surface chemical analysis—x-ray photoelectron spectrometers—calibration of energy scales, Surface and Interface Analysis: An International Journal devoted to the development and application of techniques for the analysis of surfaces, interfaces and thin films 31 (8) (2001) 721–723.
[21] G. Greczynski, L. Hultman, C 1s peak of adventitious carbon aligns to the vacuum level: dire consequences for material's bonding assignment by photoelectron spectroscopy, ChemPhysChem 18 (12) (2017) 1507.
[22] K.I. Maslakov, et al., XPS study of uranium-containing sodium-aluminum-iron-phosphate glasses, Journal of Alloys and Compounds 712 (2017) 36–43.
[23] T. Gouder, R. Eloirdi, R. Caciuffo, Direct observation of pure pentavalent uranium in U 2 O 5 thin films by high resolution photoemission spectroscopy, Scientific reports 8 (1) (2018) 1–7.
[24] B. Santos, et al., X-ray photoelectron spectroscopy study of anodically oxidized SIMFUEL surfaces, Electrochimica acta 49 (11) (2004) 1863–1873.
[25] S. Van den Berghe, et al., XPS investigations on cesium uranates: mixed valency behaviour of uranium, Journal of nuclear materials 277 (1) (2000) 28–36.
[26] V. Neck, J. Kim, Solubility and hydrolysis of tetravalent actinides, Radiochimica Acta 89 (1) (2001) 1–16.
[27] P.L. Brown, C. Ekberg, Hydrolysis of metal ions, John Wiley & Sons, 2016.
[28] I. Grenthe, et al., Studies on metal carbonate equilibria. Part 10. A solubility study of the complex formation in the uranium (VI)–water–carbon dioxide (g) system at 25°C, Journal of the Chemical Society, Dalton Transactions (11) (1984) 2439–2443.
[29] D. Shoesmith, Fuel corrosion processes under waste disposal conditions, Journal of Nuclear Materials 282 (1) (2000) 1–31.
[30] J. De Pablo, et al., The effect of hydrogen peroxide concentration on the oxidative dissolution of unirradiated uranium dioxide, MRS Online Proceedings Library Archive 663 (2000).
[31] N.L. Hansson, C. Ekberg, K. Spahiu, Alpha Dose Rate Calculations for UO2 Based Materials using Stopping Power Models, Nuclear Materials and Energy (2020) Accepted.
[32] S. Nilsson, M. Jonsson, H2O2 and radiation induced dissolution of UO2 and SIMFUEL pellets, Journal of Nuclear Materials 410 (1-3) (2011) 89–93.
[33] G.C. Allen, et al., X-ray photoelectron spectroscopy of some uranium oxide phases, Journal of the Chemical Society, Dalton Transactions (12) (1974) 1296–1301.
[34] E.S. Ilton, P.S. Bagus, Many-body effects in the 4 f x-ray photoelectron spectroscopy of the U 5+ and U 4+ free ions, Physical Review B 71 (19) (2005) 195121.
[35] J. De Pablo, et al., Solid surface evolution model to predict uranium release from unirradiated UO2 and nuclear spent fuel dissolution under oxidizing conditions, Journal of nuclear materials 232 (2-3) (1996) 138–145.
[36] Z. Zhu, J.J. Noël, D.W. Shoesmith, Hydrogen peroxide decomposition on simulated nuclear fuel bicarbonate/carbonate solutions, Electrochimica Acta (2020) 135980.
[37] P. Carbol, et al., Hydrogen suppresses UO2 corrosion, Geochimica et Cosmochimica Acta 73 (15) (2009) 4366–4375.
[38] Z. Zhu, et al., Anodic reactions occurring on simulated spent nuclear fuel (SIMFUEL) in hydrogen peroxide solutions containing bicarbonate/carbonate–The effect of fission products, Electrochimica Acta 320 (2019) 134546.
[39] E. Ekeroth, et al., Reduction of UO22+ by H2, Journal of Nuclear Materials 334 (1) (2004) 35–39.
[40] K. Spahiu, et al., The reduction of U (VI) by near field hydrogen in the presence of UO2 (s), Radiochimica Acta 92 (9-11) (2004) 597–601.
[41] A.S. Icenhour, et al., A simple kinetic model for the alpha radiolysis of water sorbed on NpO2, Nuclear technology 146 (2) (2004) 206–209.
[42] J.M. Haschke, T.H. Allen, J.L. Stakebake, Reaction kinetics of plutonium with oxygen, water and humid air: moisture enhancement of the corrosion rate, Journal of Alloys and Compounds 243 (1-2) (1996) 23–35.
[43] P.A. Korzhavyi, et al., Oxidation of plutonium dioxide, Nature Materials 3 (4) (2004) 225–228.